

Hydrogen/Syngas Production from Different Types of Waste Plastics Using a Sacrificial Tire Char Catalyst via Pyrolysis–Catalytic Steam Reforming

Yukun Li, Mohamad A. Nahil, and Paul T. Williams*



Cite This: *Energy Fuels* 2023, 37, 6661–6673



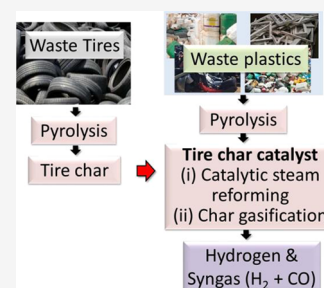
Read Online

ACCESS |

Metrics & More

Article Recommendations

ABSTRACT: Single plastics and mixed waste plastics from different industrial and commercial sectors have been investigated in relation to the production of hydrogen and syngas using a pyrolysis–catalytic steam reforming process. The catalyst used was a carbonaceous char catalyst produced from the pyrolysis of waste tires. Total gas yields from the processing of single plastics were between 36.84 and 39.08 wt % (based on the input of plastic, reacted steam, and char gasification) but those in terms of the gas yield based only on the mass of plastic used were very high. For example, for low-density polyethylene (LDPE) processing at a catalyst temperature of 1000 °C, the gas yield was 445.07 wt % since both the reforming of the plastic and also the steam gasification of the char contributed to the gas yield. The product gas was largely composed of H₂ and CO, i.e., syngas (~80 vol %), and the yield was significantly increased as the char catalyst temperature was raised from 900 to 1000 °C. Hydrogen yields for the processing of the polyolefin single plastics were ~130 mmol g_{plastic}⁻¹ at a catalyst temperature of 1000 °C. The pyrolysis–catalytic steam reforming of the industrial and commercial mixed plastics with the tire char catalyst produced hydrogen yields that ranged from 92.81 to 122.6 mmol g_{plastic}⁻¹ and was dependent on the compositional fraction of the individual plastics in their mixtures. The tire char catalyst in the process acted as both a catalyst for the steam reforming of the plastics pyrolysis volatiles to produce hydrogen and also as a reactant (“sacrificed”), via carbon-steam gasification to produce further hydrogen.



1. INTRODUCTION

The service lifetimes of plastics in different end-use applications can range from only weeks for plastic packaging and 5–20 years for automotive industry plastics to >50 years for building and constructing plastics.^{1,2} A recent review of the global lifecycle material flow of plastics and their impact on the environment reported that the generation of waste plastics was estimated to be more than 350 million tonnes per year.¹ Importantly, for the environment, more than 23 wt % of global waste plastics are categorized as “mismanaged,” of which a large proportion (22 million tonnes/year (Mt/y)) enters the environment, causing pollution and potential damage to health.^{1,3} The major commercial and industrial sectors contributing to the 470 Mt/y global production of new plastics include 142 Mt/y from packaging, 47 Mt/y from consumer products, 44 Mt/y from the textile sector (e.g., clothing etc.), 54 Mt/y from the transport sector, 77 Mt/y from the building and construction industry, and 17 Mt/y from electronic and electrical wastes.¹ These sectors generate huge tonnages of plastic waste, which instead of being considered as a waste problem, have a massive potential for exploitation as a feedstock resource for the production of higher-value products.

One such higher-value product is hydrogen. Global production of hydrogen in 2021 was 94 million tonnes with the main uses in oil refining and industrial uses such as

chemical production and iron and steel manufacture.⁴ In response to climate change, the demand for hydrogen in heavy-duty road and marine and aviation sectors in power production and for decarbonizing heavy industry (e.g., iron and steel) is predicted to grow, with estimates of demand for hydrogen at 200 million tonnes/year by 2030 and 500 million tonnes/year by 2050.⁴ The production of hydrogen is currently almost entirely from fossil fuel feedstocks, with the catalytic steam reforming of natural gas methane, the dominant process. Producing hydrogen from waste plastics would be an alternative to using natural gas and coal; also, in that plastics are largely produced from fossil fuel petroleum. Fossil fuel resources would be conserved by recycling the plastics.

There has been much research into the production of hydrogen from waste plastics involving thermochemical routes, including pyrolysis and gasification, and several different process configurations have been investigated and recently reviewed.^{5–10} A successful two-stage pyrolysis–catalytic steam

Received: February 15, 2023

Revised: March 29, 2023

Published: April 12, 2023



Table 1. Ultimate and Proximate Analysis of the Plastic Materials^a

sample	ultimate analysis (wt %)					proximate analysis (wt %)		
	N	C	H	O	S	volatile	fixed carbon	ash
HDPE	0.37	80.26	15.33	4.04	nd	93.64	0.16	6.66
LDPE	0.37	83.17	16.34	0.12	nd	95.93	0.10	5.52
PP	0.36	82.03	16.55	1.07	nd	95.30	0.03	6.04
PS	0.42	86.09	7.87	5.63	nd	95.43	0.15	5.52
PET	0.32	60.31	3.95	35.43	nd	81.92	14.85	4.51
MP _{SIM}	0.37	79.51	13.04	7.08	nd	93.25	2.32	5.64
MP _{MW}	0.89	63.89	5.27	29.95	nd	84.39	13.26	1.20
MP _{HP}	1.09	81.49	10.57	6.85	nd	89.64	8.35	0.84
MP _{CONST}	0.64	81.85	11.38	6.12	nd	93.96	5.16	0.14
MP _{AGRIC}	1.23	80.76	10.89	7.13	nd	94.78	4.44	0.14
MP _{MSW}	0.76	80.50	11.04	7.70	nd	92.39	6.11	0.34

^and = Not detected.

reforming process for the production of hydrogen from waste plastics has been developed and investigated by several different research groups.^{11–14} The pyrolysis–catalytic reforming process involves initial pyrolysis of the plastics in the first stage to produce a wide range of volatile hydrocarbons, which are subsequently catalytically steam-reformed in the second stage. The two stages are usually separate reactors to aid independent process control of the reaction parameters to optimize both the pyrolysis and reforming stages.¹² In addition, there has been extensive investigation of different types of catalyst to optimize the reforming stage, as reported and reviewed in detail by Santamaria et al.⁹ Nickel-based catalysts are the most commonly investigated catalyst for the pyrolysis–catalytic steam reforming of waste plastics because of their catalytic activity for hydrocarbon reforming, moderate cost, and mechanical strength and not least because they have been widely investigated and developed for the commercial catalytic steam reforming of natural gas.¹⁵ Various nickel-based catalysts have been investigated to maximize hydrogen yield from the pyrolysis–catalytic steam reforming of plastics, in terms of added metal promoters,^{16,17} in terms of the influence of different support materials,¹³ and also the method of catalyst preparation,¹⁸ while others have used commercially available nickel–alumina catalysts such as C11-NK¹⁹ and G90 LDP.⁹ For nickel-based catalysts, the catalytic temperatures are typically 800–900 °C.^{13,20–22}

Several researchers have focused on the use of pyrolysis char as catalysts to enhance hydrogen production and to remove gasification tars.^{23–25} For example, Wang et al.²⁶ reported that the gas yield increased from 29.6 to 35.0 wt % by using municipal solid waste (MSW) pyrolysis char as a catalyst for reforming the pyrolysis volatiles from MSW. Biochar produced from the pyrolysis of biomass has also been used as a catalyst. The alkaline-earth metal oxides (CaO and MgO) contained in the biomass pyrolysis char have been shown to have a catalytic function in relation to tar cracking during the steam gasification of biomass.²⁷ In addition, the chemical structure of biochar, especially the O-containing functional groups, play an important role in the steam reforming of volatiles in the presence of biochar.^{28,29} We have previously reported the use of pyrolysis char derived from the pyrolysis of waste tires as a catalyst for the reforming of hydrocarbons produced from the pyrolysis of biomass, where the char acts as both a reforming catalyst and also as a reactant for the production of hydrogen and carbon oxides through steam gasification.³⁰ Thereby, the carbonaceous char is “sacrificed” during the reaction with the

aim of generating higher yields of hydrogen and syngas (H₂ and CO). The tire char was shown to contain high concentrations of transition metals, for example, Zn, Fe, Co, and Cu that acted as active reforming catalyst metals. However, there are few reports on the use of tire pyrolysis-derived char as a catalyst for the pyrolysis–catalytic steam reforming of waste plastics.

In the work reported here, we investigate the production of hydrogen from several different types of single plastics typically found in municipal solid waste (high density polyethylene (HDPE), low-density polyethylene (LDPE), polypropylene (PP), polystyrene (PS), and poly(ethylene terephthalate) (PET)). A mixture of the single plastics was also processed in proportions typically found in municipal solid waste. In addition, mixed “real-world” waste plastics from drinks bottles, household packaging, construction waste, agricultural waste, and mixed municipal solid waste were investigated. The plastics were processed in a laboratory scale, two-stage fixed bed reactor using pyrolysis–catalytic steam reforming with tire-derived pyrolysis char as the “sacrificial” catalyst.

2. MATERIALS AND METHODS

2.1. Materials. The single plastics used in the experiments were HDPE, LDPE, PP, PS, PET, and their mixture (MP_{SIM}), whose composition was based on an estimate of residual waste plastics found in municipal solid waste as reported by Delgado et al.³¹ with plastic contents of LDPE, 41 wt %; HDPE, 19 wt %; PS, 15 wt %; PET, 15 wt %; and PP, 10 wt %. In addition, several “real-world” commercial and industrial waste plastics were also investigated, consisting of mixed plastics from mineral water bottle packaging (MP_{MW}), household packaging (MP_{HP}), construction waste (MP_{CONST}), agriculture waste plastics (MP_{AGRIC}), and mixed plastics from municipal solid waste (MP_{MSW}). Table 1 shows the ultimate and proximate analysis of the plastics.

The tire char catalyst was prepared from waste tires by pyrolysis using a fixed bed reactor. The reactor used was a stainless steel reactor (40 mm diameter, 200 mm height). The tire pyrolysis was undertaken under nitrogen, where the tire was heated from 20 to 800 °C at 20 °C min⁻¹ heating rate to produce a char yield of 36.5 wt %. The concentration of specific elements in the prepared tire char was determined by ashing the char and then acid digestion of the ash in nitric acid at 240 °C, followed by atomic absorption analysis (Varian AA240FS).

The tire char was also analyzed to determine the Brunauer–Emmett–Teller (BET) surface area with a Micrometrics Tristar 3000 apparatus, which also enabled the pore size distribution to be calculated (Barrett–Joyner–Hallender method). The surface morphology and metal content of the char was determined by coupled

scanning electron microscopy (SEM)–energy-dispersive X-ray spectrometry (EDXS) with a Hitachi SU8230 SEM and Oxford Instruments Aztec Energy EDXS.

2.2. Experimental Reactor System. The two-stage experimental pyrolysis–catalytic steam reforming reactor system is shown in Figure 1. Waste plastic samples (1.0 g) were placed in a steel crucible and

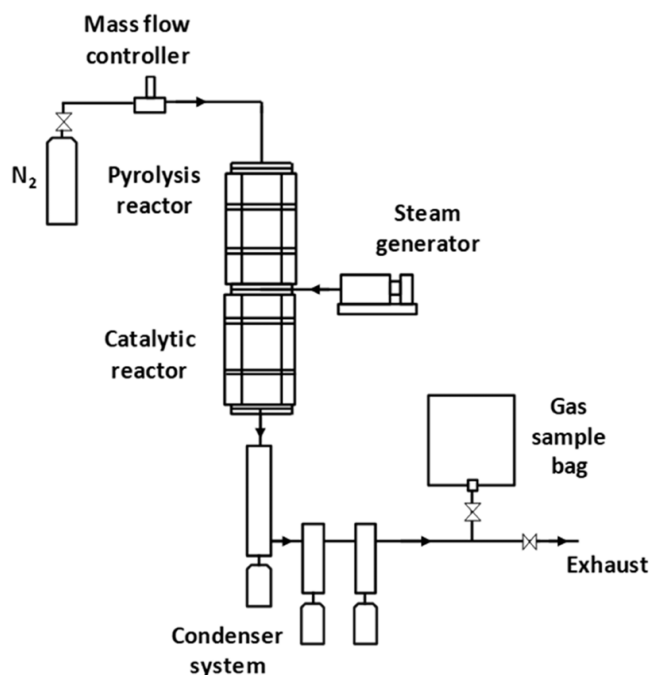


Figure 1. Schematic diagram of the two-stage pyrolysis–catalytic steam reforming reaction system.

pyrolyzed in the first-stage pyrolysis reactor, heating from 40 °C min⁻¹ to a final temperature of 500 °C. Evolved pyrolysis hydrocarbons passed to the second-stage catalyst reactor containing the tire char catalyst (1.0 g), which was heated to either 900 or 1000 °C. The tire char catalyst temperatures of 900 and 1000 °C were chosen since our preliminary work showed that the yield of hydrogen at catalyst reforming temperatures, which have typically been used previously, of 800–850 °C^{13,22} produced only low levels of hydrogen. For example, we obtained only 26.93 mmol H₂ g_{plastic}⁻¹ at a tire char catalyst reforming temperature of 800 °C for HDPE, which was much lower than that reported in this work. Steam was introduced into the catalyst reactor via a water pump at a flow rate of 8 mL h⁻¹. The gases produced from the pyrolysis–catalytic process such as H₂ and CO reduced the metal oxides contained in the char in situ to metal elements, which played a catalytic role in cracking the pyrolysis

volatiles. Evolved product gases from the process were collected in a gas sample bag and were analyzed immediately after each experiment using packed column gas chromatography using three separate Varian 3380 gas chromatographs configured for either permanent or hydrocarbon gases.³² Hydrocarbon gases C₁–C₄ were analyzed on a HayeSep 80–100 mesh column, N₂ mobile phase, and a flame ionization detector (FID); H₂, O₂, N₂, and CO were analyzed with a 60–80 mesh molecular sieve column, Ar carrier gas, and a thermal conductivity detector (TCD); CO₂ was analyzed on a 80–100 mesh HayeSep column, Ar carrier gas, and TCD. Gases were determined by mass calculated from gas concentrations, gas flow rates, and the ideal gas law.

The standard gas used for the calibration of permanent gas and CO₂ consisted of a 1% volumetric concentration of H₂, O₂, CO, CO₂, and 96% N₂ (mole percentage content). The standard gas for hydrocarbon gas calibration consisted of a 1% volumetric concentration of CH₄, C₂H₄, C₂H₆, C₃H₆, C₃H₈, C₄H₈, C₄H₁₀, and 93% N₂. The standard gas peak areas corresponding to each standard gas were obtained using Varian Star software (Varian Ltd. U.K.) to calculate the concentration of each gas in the product gas based on eq 1

$$C_{\text{sample}} = \frac{C_{\text{standard}} \times P_{\text{sample}}}{P_{\text{standard}}} \quad (1)$$

where C_{sample} represents the concentration of the sample gas, C_{standard} represents the concentration of the standard gas, P_{sample} represents the peak area of the sample gas obtained from the gas chromatograph (GC), and P_{standard} represents the peak area of the standard gas obtained from the GC.

Each gas yield was calculated by the molar percentage content of each gas and the molar percentage content of the nitrogen carrier gas based on the following equations

$$V_{\text{total gas}} = \frac{F_{\text{N}_2} \times T}{C_{\text{N}_2}} \quad (2)$$

$$V_{\text{each gas}} = V_{\text{total gas}} \times C_{\text{each gas}} \quad (3)$$

$$M_{\text{each gas}} (\text{g}) = \frac{V_{\text{each gas}} \times \text{molar}_{\text{each gas}}}{22.4} \quad (4)$$

$$\text{gas yield} = \frac{\sum M_{\text{each gas}}}{m_{\text{plastic}} + m_{\text{water}} + m_{\text{reacted char}}} \quad (5)$$

$$\text{H}_2 \text{ yield} (\text{mmol g}_{\text{plastic}}^{-1}) = \frac{V_{\text{H}_2}}{22.4} / m_{\text{plastic}} \quad (6)$$

where $V_{\text{total gas}}$ represents the total gas collected in gas sample bag, F_{N_2} represents the flow rate of N₂, T represents the gas collection time, C_{N_2} represents the gas concentration of N₂, $V_{\text{each gas}}$ represents the volume of each gas, $C_{\text{each gas}}$ represents the gas concentration of each

Table 2. Characteristics of the Tire Char Catalyst

tire char catalyst					
ash content (wt %)	14.72				
elemental analysis (wt %)				metal content (wt %)	
carbon	79.02			zinc	7.43
hydrogen	0.66			silicon	2.20
oxygen	16.58			calcium	0.53
nitrogen	0.29			magnesium	0.13
sulfur	3.46			potassium	0.12
				iron	0.44
				copper	0.04
				cobalt	0.12
surface area (m ² g ⁻¹)	micropore surface area (m ² g ⁻¹)	mesopore surface area (m ² g ⁻¹)	average pore size (nm)	cumulative pore volume (mL g ⁻¹)	
79.07	9.25	69.82	22.75	0.57	

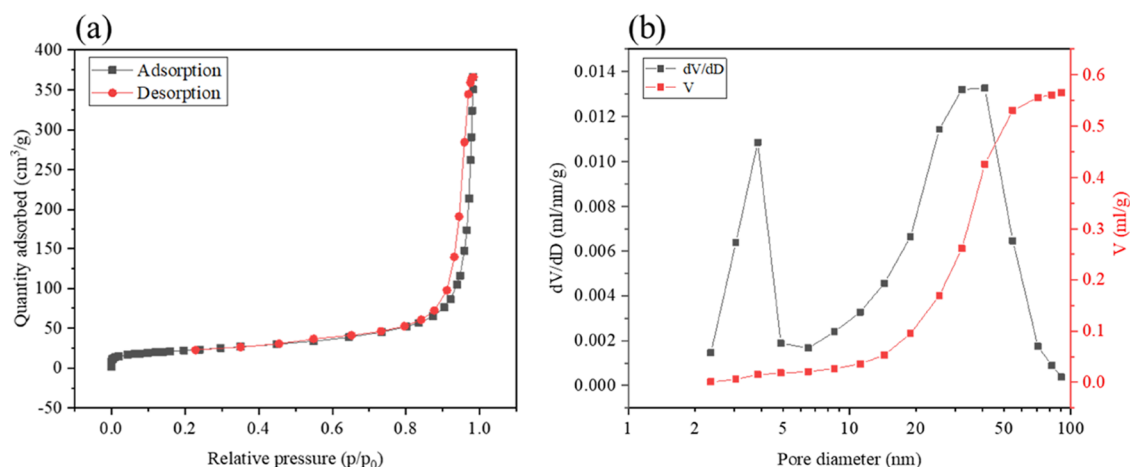


Figure 2. (a) N_2 adsorption–desorption isotherms and (b) pore size distribution of the char catalyst.

gas, $M_{\text{each gas}}$ represents the mole of each gas, $M_{\text{each gas}}$ represents the mass of each gas, m_{plastic} represents the mass of plastic, m_{water} represents the mass of water, and $m_{\text{reacted char}}$ represents the mass of reacted char.

3. RESULTS AND DISCUSSION

3.1. Characterization of the Tire Char Catalyst. Table 2 shows the characteristics of the waste tire-derived tire pyrolysis char catalyst. The char ash content was 14.72 wt % with a high sulfur content (3.46 wt %). The metals present in the ash included high concentrations of transition metals (e.g., Zn, Fe, Cu, Co), which have been investigated for the catalytic steam reforming process applied to waste plastics.⁹ The high concentrations of zinc and sulfur are related to the additives used in tire manufacture, the zinc used in the tire rubber vulcanization process and to enhance physical properties, and the sulfur used to cross-link the rubber polymer chains and part of the tire hardening process.³³ The presence of high concentrations of silicon, calcium, magnesium, potassium, and iron are associated with the use of clay as a filler material in the tire manufacturing process. Since the original tire used to prepare the char catalyst was a waste material, significant metal contamination may also be present adhered to the tire.

Table 2 also shows the surface area and pore size characteristics of the prepared tire char catalyst. The tire char catalyst contained a large number of mesopores (2–50 nm), which can be demonstrated by the surface area of the micropores and mesopores. The surface area of the fresh tire char catalyst was $79.07 \text{ m}^2 \text{ g}^{-1}$, with the surface area of mesopores contributing 88% and micropores contributing 12% of the total surface area. Figure 2 shows the nitrogen adsorption–desorption isotherms (Figure 2a) and the pore size distribution of the tire char catalyst (Figure 2b). From Figure 2a, it can be seen that, starting from the relative pressure of 0.4, the adsorption volume of the desorption process is higher than that of the adsorption process, which is mainly because of the capillary adsorption. In addition, Figure 2b shows that the pore diameter corresponding to the peak value of dV/dD occurred at 4 nm and also at 30–40 nm, which also indicated that the pore structure of the tire char was mostly mesoporous. The wide distribution of these mesopores (20–50 nm) made the cumulative adsorption volume reach $0.57 \text{ cm}^3 \text{ g}^{-1}$, and the average adsorption pore diameter was 22.75 nm.

SEM-EDXS elemental mapping was carried out on the raw tire rubber, prepared tire char catalyst, and the used tire char to determine the change of surface morphology and distribution of the major metals and also sulfur on the surface of the char. The results are shown in Figure 3. Figure 3a–e shows the surface morphology of the raw tire rubber and the distribution of Fe, Zn, Mg, and Ca metals on the original tire. The bright spots in the figure indicated a high metal content. It can be observed that the surface of the tire was regular and relatively smooth, and the metal content was scattered sporadically on the surface of the tire, among which zinc was abundant and was well dispersed. The SEM image and metal distribution of the prepared tire char are shown in Figure 3f–k. Figure 3f shows the morphology of the fresh tire char catalyst, which demonstrated an uneven structure. The pyrolysis process devolatilized the tire, resulting in some metal elements being exposed on the surface of the tire char. Some of the small metal particles were agglomerated into larger particles (the brighter large particles in Figure 3f). Figure 3g–k shows the elemental distribution of some of the major elements (S, Na, Zn, Fe, Ca) found in the tire char. The micrographs shown in Figure 3i,g show that the zinc and sulfur were widely distributed in the tire char and existed in the same locations, suggesting that they were present in the form of ZnS. The distribution of Na, Fe, and Ca is shown in Figure 3h,j,k; Zhou et al. reported that Na, Fe, and Ca in char prepared from waste tires existed in the form of oxides.³⁴ Figure 3l–n shows the characterization of the used tire char catalyst recovered after the experiments carried out at $1000 \text{ }^\circ\text{C}$ reforming temperature. The surface of the recovered catalyst became flat and smooth, and only Fe and Ca were detected, indicating that the tire char ash content was rich in Fe and Ca compounds. The dissociative sublimation of ZnS in the tire char occurs at high temperature to produce Zn and S_x , which reacted with steam to produce ZnO, H_2S , SO_2 , and H_2 during steam gasification.³⁵ At $1000 \text{ }^\circ\text{C}$ char catalyst temperature, the Zn released by ZnS was completely volatilized, resulting in no Zn being present on the catalyst surface.

3.2. Pyrolysis–Catalytic Steam Reforming of Individual Plastics. 3.2.1. *Product Yields from Pyrolysis–Catalytic Steam Reforming of Different Plastics.* The product yields from pyrolysis–catalytic steam reforming of different plastics at catalytic steam reforming temperatures of 900 and $1000 \text{ }^\circ\text{C}$ are shown in Table 3. The data are presented in terms of the

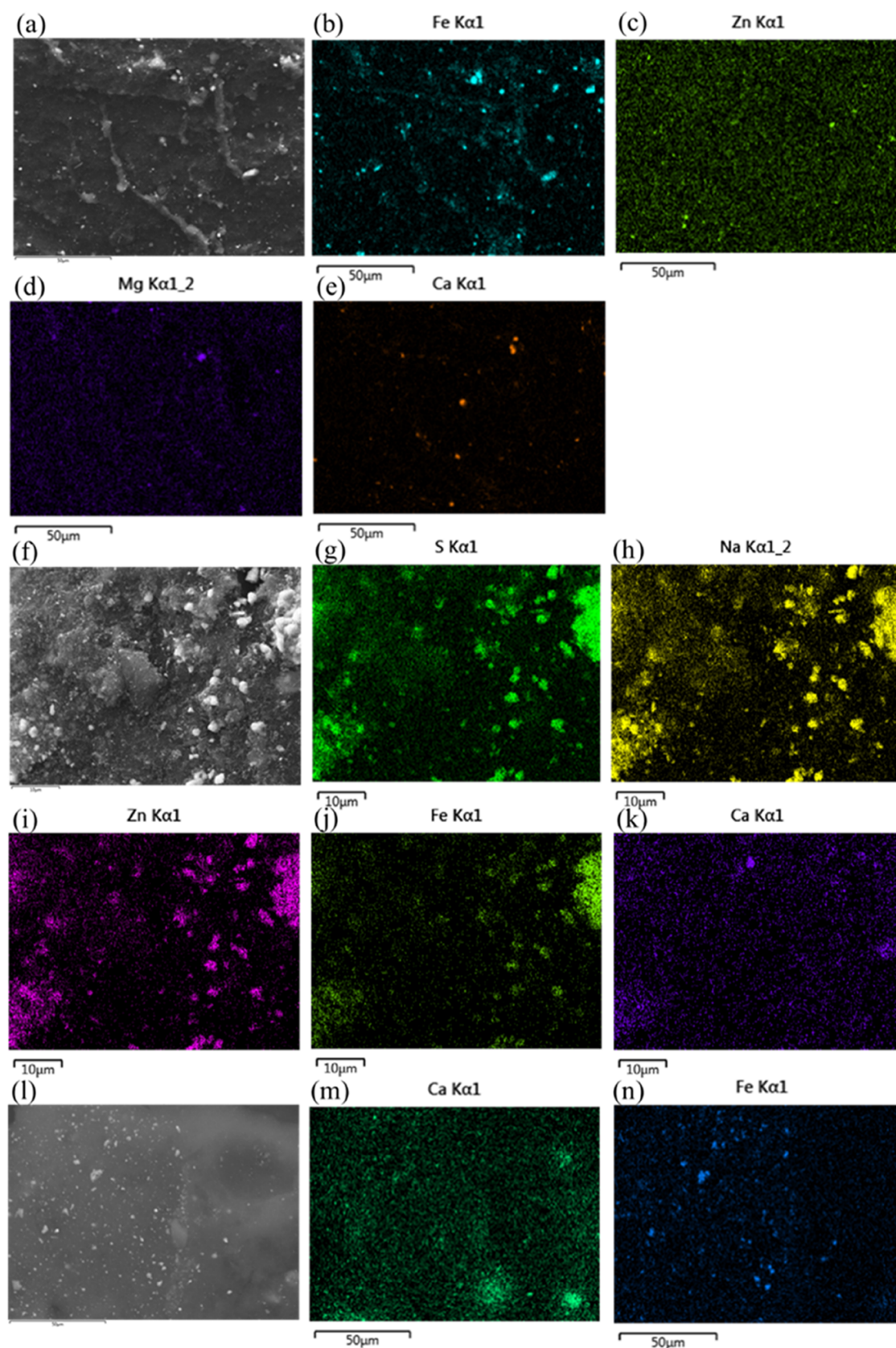


Figure 3. SEM images of the tire, prepared tire pyrolysis char catalyst, and used tire char catalysts coupled with elemental mapping ((a–e) SEM image and elemental mapping of tire, (f–k) SEM image and elemental mapping of the char catalyst, and (l, n) SEM image and elemental mapping of used char catalysts).

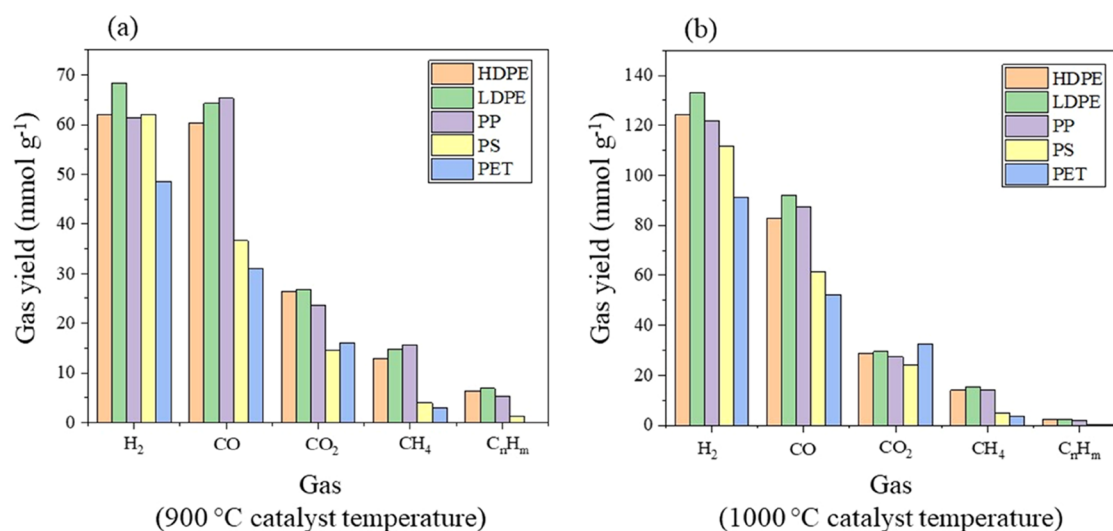
Table 3. Product Yields from Pyrolysis–Catalytic Steam Reforming of Different Plastics at 900 and 1000 °C

	HDPE	LDPE	PP	PS	PET
Char Catalyst Temperature 900 °C					
yield based on the sample + water + reacted char					
gas yield (wt %)	36.84	39.08	37.08	21.27	18.71
liquid yield (wt %)	65.94	68.17	68.08	70.03	68.47
gas yield based on the plastic sample (wt %)	337.44	356.03	340.43	189.47	172.76
char catalyst reacted (g)	0.36	0.33	0.34	0.24	0.4
reacted water (g)	1.76	1.57	1.59	1.43	1.51
Char Catalyst Temperature 1000 °C					
yield based on the sample + water + reacted char					
gas yield (wt %)	43.47	46.80	43.31	33.47	33.03
liquid yield (wt %)	52.42	51.31	53.68	56.34	54.19
gas yield based on the plastic sample (wt %)	412.94	445.07	418.03	308.97	319.36
char reacted (g)	0.75	0.75	0.75	0.65	0.86
reacted water (g)	2.77	2.88	2.72	2.38	2.57

product yield based on the mass of product divided by the total mass of the input plastic, reacted water, and reacted char; in addition, also shown is the gas yield based on the input of only the mass of plastic. There was negligible residual pyrolysis char (<0.5 wt %) found in the first-stage pyrolysis reactor after experimentation for the pyrolysis of LDPE, HDPE, PP, and PS, with almost complete transformation into gas. However, PET produced a significant amount, ~17 wt %, of residual char as has been reported before.³⁶ In addition, it should be noted that the liquid denoted in Table 3 is composed of condensed water from the steam input, i.e., unreacted steam, and there was only negligible product oil formed (<0.5 wt %). Table 3 shows that, for the 900 °C char catalyst reforming temperature, the gas yield for pyrolysis–catalytic steam reforming of LDPE based on the input of plastic, water, and reacted char was the highest, at 39.08 wt %. Under the same conditions, similar gas yields were obtained for HDPE and PP, but much lower gas yields were obtained for PS and PET. The low product yields for PS

and PET are related to the chemical structure of those plastics; there are functional groups on the polymerization skeleton of PET and PS, which is conducive to depolymerization into monomers, such as benzoic acid, styrene, etc., and these compounds have a low conversion rate in the catalytic process.³⁷ However, the pyrolysis of PE and PP is mainly random chain scission, with similar compositions of the volatiles derived from their pyrolysis; therefore, these volatiles will react similarly in the second catalytic steam reforming stage. In the tire char catalytic reforming of HDPE, LDPE, and PP, about 0.35 g of the original 1.0 g of tire char was reacted. However, the consumption of tire char in the catalytic reforming of PS and PET was 0.24 and 0.4 g, respectively, indicating that PS pyrolysis volatiles inhibited tire char gasification, while PET pyrolysis volatiles promoted tire char gasification.

Table 3 also shows the product yields from pyrolysis–catalytic steam reforming of different plastics produced at a char catalyst temperature of 1000 °C. By comparing the gas yields based on the sample, water, and reacted char at different temperatures, it was calculated that the gas yields from pyrolysis–catalytic steam reforming of HDPE, LDPE, and PP were increased by about 7 wt %. The gas yields from pyrolysis–catalytic steam reforming of PS and PET were increased by 12 and 14 wt %, respectively, when the temperature was increased from 900 to 1000 °C. There are two main reasons for the increase in gas production; one is that, at higher temperatures, hydrocarbons react more easily with steam in the presence of metals in the tire char; the other is that the carbon in the tire char reacts with more steam, resulting in more H₂ and CO production. This is also the reason for the increased water consumption (reacted water) in the catalytic steam reforming process. Similar to the results found at 900 °C catalyst temperature, the gas yield from catalytic pyrolysis of LDPE at 1000 °C was the highest among the single plastics investigated, at 46.80 wt %. In relation to the tire char consumption by steam gasification reactions, the tire char reacted the most in the processing of PET with 0.86 g of the original 1.0 g of tire char being consumed/ reacted during pyrolysis–catalytic steam reforming.

**Figure 4.** Individual gas yield from pyrolysis–catalytic steam reforming of individual plastics at a char catalyst temperature of (a) 900 °C and (b) 1000 °C.

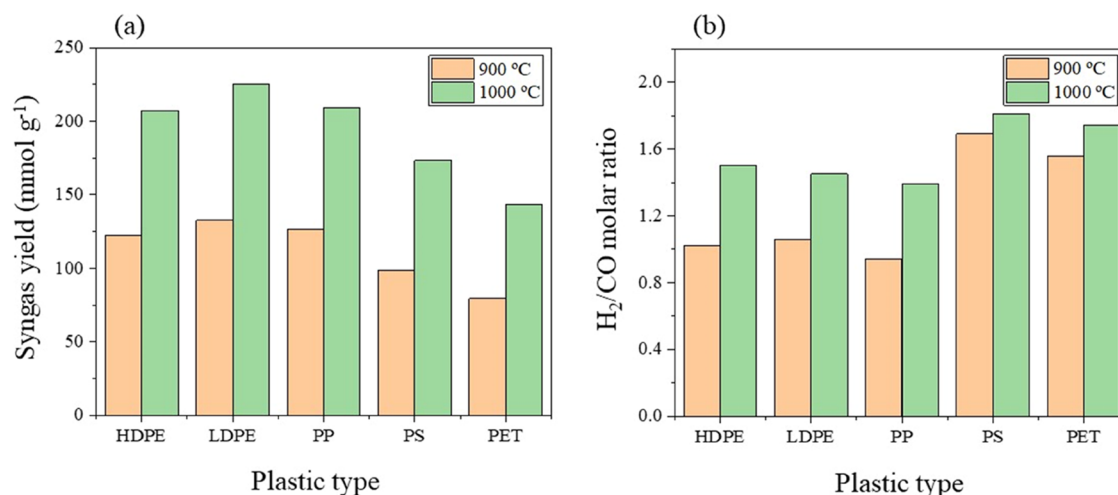


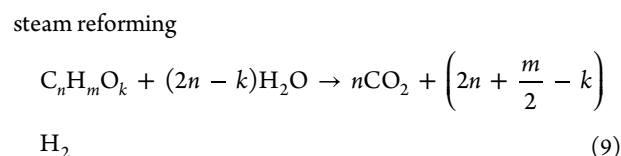
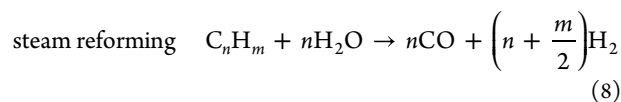
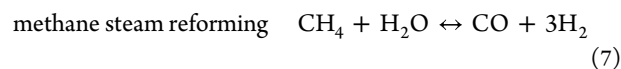
Figure 5. (a) Syngas yield ($\text{H}_2 + \text{CO}$) and (b) H_2/CO molar ratio from pyrolysis–catalytic steam reforming of individual plastics in relation to char catalyst temperatures of 900 and 1000 °C.

3.2.2. Gas Yields from Pyrolysis–Catalytic Steam Reforming of Single Plastics. The individual gas yields from pyrolysis–catalytic steam reforming of HDPE, LDPE, PP, PS, and PET at tire char catalyst temperatures of 900 and 1000 °C are shown in Figure 4. At 900 °C char catalyst temperature, the H_2 yield from processing LDPE was the highest at 68.29 $\text{mmol g}_{\text{plastic}}^{-1}$, followed by HDPE, PP, and PS at about 62 $\text{mmol g}_{\text{plastic}}^{-1}$, while the yield of PET was the lowest at 48.55 $\text{mmol g}_{\text{plastic}}^{-1}$. The low H_2 yield from PET is due to the production of a high carbonaceous residue yield of 17 wt % obtained from the pyrolysis stage, with a consequent low yield of gases for reforming in the second-stage catalytic reactor. In addition, the chemical structure of PET and associated thermal degradation behavior differed from other polyolefin plastics.³⁶ The CO yield from the pyrolysis–catalytic steam reforming of HDPE, LDPE, and PP was more than 60 $\text{mmol g}_{\text{plastic}}^{-1}$; however, CO yields from processing PS and PET were lower at 36.61 $\text{mmol g}_{\text{plastic}}^{-1}$ and 31.08 $\text{mmol g}_{\text{plastic}}^{-1}$, respectively. Given the similar elemental composition and chemical structure of HDPE, LDPE, and PP, there was only a small difference in the gases produced by the reforming of volatiles produced from these plastics. Compared with HDPE, LDPE, and PP, the gas yields from PS and PET were significantly different, with low yields of hydrocarbon gases.

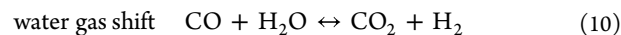
At the catalyst temperature of 1000 °C, the H_2 yield from the pyrolysis–catalytic steam reforming of the different single plastics was almost twice that produced at the catalyst temperature of 900 °C. LDPE produced the highest H_2 yield at 133.10 $\text{mmol g}_{\text{plastic}}^{-1}$, while PET produced the lowest H_2 yield, at 91.16 $\text{mmol g}_{\text{plastic}}^{-1}$. The CO yield from the different plastics was increased by more than 20 $\text{mmol g}_{\text{plastic}}^{-1}$ when the catalyst temperature was increased to 1000 °C, for example, the CO yield from LDPE increasing the most to produce 92.03 $\text{mmol g}_{\text{plastic}}^{-1}$. The CO_2 yield from pyrolysis–catalytic steam reforming of HDPE, LDPE, and PP increased slightly, while the CO_2 yield of PS increased by 9.4 $\text{mmol g}_{\text{plastic}}^{-1}$, and the yield from PET was increased by 16.39 $\text{mmol g}_{\text{plastic}}^{-1}$. The CH_4 generated from the pyrolysis–catalysis steam reforming of all of the single plastics increased by about 1 $\text{mmol g}_{\text{plastic}}^{-1}$, compared with the results produced at 900 °C. The CH_4 mainly came from the gasification of tire char since preliminary

experiments using only tire char gasification under steam showed that about 1 $\text{mmol g}_{\text{plastic}}^{-1}$ of CH_4 could be generated.

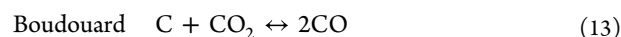
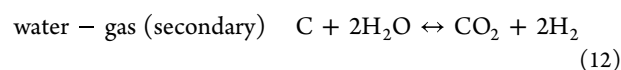
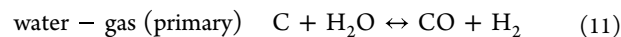
The reaction of the pyrolysis hydrocarbon volatiles (eqs 7 and 8) from the polyolefin (HDPE, LDPE, PP) and polystyrene volatiles with steam and the PET volatiles (eq 9) with steam are shown below.



In addition, further reactions of the product carbon monoxide may occur via the water gas shift reaction



Also, the carbon content of the tire pyrolysis char will also be involved in steam gasification reactions



The increase of H_2 yield when the catalytic temperature is increased has been reported in the pyrolysis–catalytic steam reforming of various plastics at 800 and 850 °C using an Ni–Mg–Al catalyst.³⁸ In the pyrolysis–catalytic steam reforming of biomass for hydrogen production (eqs 6–9), tire char has been shown to promote the water gas shift reaction (eq 10) at high temperatures, thus increasing H_2 concentration.³⁰ Franco et al.³⁹ also showed that the water gas shift reaction was promoted when the temperature was higher than 700 °C, resulting in an increase in H_2 concentration.

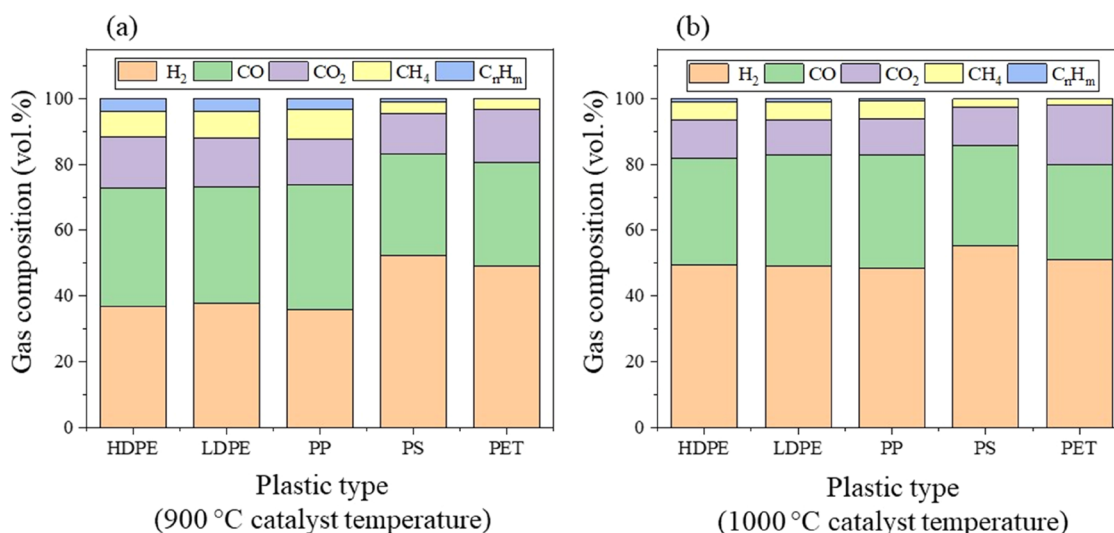


Figure 6. Gas composition (vol %) for pyrolysis–catalytic steam reforming of individual plastics at a char catalyst temperature of (a) 900 °C and (b) 1000 °C.

Table 4. Product Yields from Pyrolysis–Catalytic Steam Reforming of Mixed Plastics at 1000 °C

plastics	MP _{MW}	MP _{HP}	MP _{CONST}	MP _{AGRIC}	MP _{MSW}	MP _{SIM}
yield based on the sample + water + reacted char						
gas yield (wt %)	30.61	41.94	41.67	43.47	40.44	37.50
liquid yield (wt %)	56.77	54.98	52.70	52.74	56.47	52.06
gas yield based on the plastic sample (wt %)	282.50	387.52	385.05	412.93	387.43	354.37
char reacted (g)	0.75	0.69	0.71	0.72	0.68	0.66
reacted water (g)	2.24	2.47	2.66	2.77	2.49	2.87

3.2.3. Syngas Yield and H₂/CO Molar Ratio from Pyrolysis–Catalytic Steam Reforming of Individual Plastics. Syngas consists of H₂ and CO and is considered a major energy source with applications in various industrial sectors. Syngas produced with different H₂/CO molar ratios can be used for various purposes; for example, syngas with high H₂/CO molar ratios can be used to produce hydrogen for synthetic ammonia production or for use in fuel cells.⁴⁰ Low-H₂/CO-molar ratio syngas is an ideal feedstock for the Fischer–Tropsch process to produce transportation fuel.⁴¹ Figure 5a shows the syngas yield for the pyrolysis–catalytic steam reforming of individual plastics at tire char catalyst temperatures of 900 and 1000 °C. As seen in Figure 5a, when the catalyst temperature was increased from 900 to 1000 °C, the syngas yield calculated in terms of the plastic processed produced from each plastic increased significantly. The highest syngas yield was produced by LDPE at 225.13 mmol g_{plastic}⁻¹ for the steam reforming experiment undertaken at a char catalyst temperature of 1000 °C compared with 132.56 mmol g_{plastic}⁻¹ for the experiment at a catalyst temperature of 900 °C.

The H₂/CO molar ratios produced from the pyrolysis–catalytic steam reforming processing of the different single plastics at catalyst temperatures of 900 and 1000 °C are shown in Figure 5b. It can be seen that the H₂/CO molar ratio of the gas products produced from PS and PET was higher than that of the polyolefin plastics. The H₂/CO molar ratio of all of the different types of plastics increased with the increase in catalyst temperature from 900 to 1000 °C. This was mainly because, at higher temperatures, the steam reforming reaction of hydrocarbons was enhanced. Al-Rahbi and Williams³⁰ also found that the H₂/CO molar ratio increased with the increase of

catalyst temperature in the gas products produced from the pyrolysis–catalytic steam reforming of biomass using tire char as a catalyst.

3.2.4. Volumetric Gas Composition from Pyrolysis–Catalytic Steam Reforming of Single Plastics. The volumetric gas compositions obtained for the pyrolysis–catalytic steam reforming of HDPE, LDPE, PP, PS, and PET at tire char catalyst temperatures of 900 and 1000 °C are shown in Figure 6a,b, respectively. As can be seen from Figure 6a, the H₂ concentration from the processing of HDPE and LDPE with a catalyst temperature of 900 °C was similar at about 38 vol %, with H₂ concentration from processing PP slightly lower than that for HDPE and LDPE at 36 vol %. Although the total gas yield of PS and PET was lower than the other three plastics (Table 3), the relative volumetric H₂ concentration in the product gas was higher, at 52.4 and 49.1 vol %, respectively. The pyrolysis volatiles from HDPE, LDPE, and PP were mainly hydrocarbons (C_nH_m), while the pyrolysis volatiles from PS were largely aromatic hydrocarbons, and the pyrolysis volatiles of PET were oxygenated hydrocarbons (C_nH_mO_k).³⁷ These compositions of plastics pyrolysis gases influence the final product gas from the combined pyrolysis–catalytic steam reforming process.

Increasing the temperature of the tire char catalyst to 1000 °C (Figure 6b), showed that the relative volumetric concentration of H₂ in the gas products from the pyrolysis–catalytic steam reforming of HDPE, LDPE, and PP was increased from 36–38 to ~49 vol %. The concentration of H₂ in PS and PET pyrolysis gas was not significantly increased as the catalyst temperature was increased and the content of C_nH_m was less than 1 vol %. So a large part of the increase in

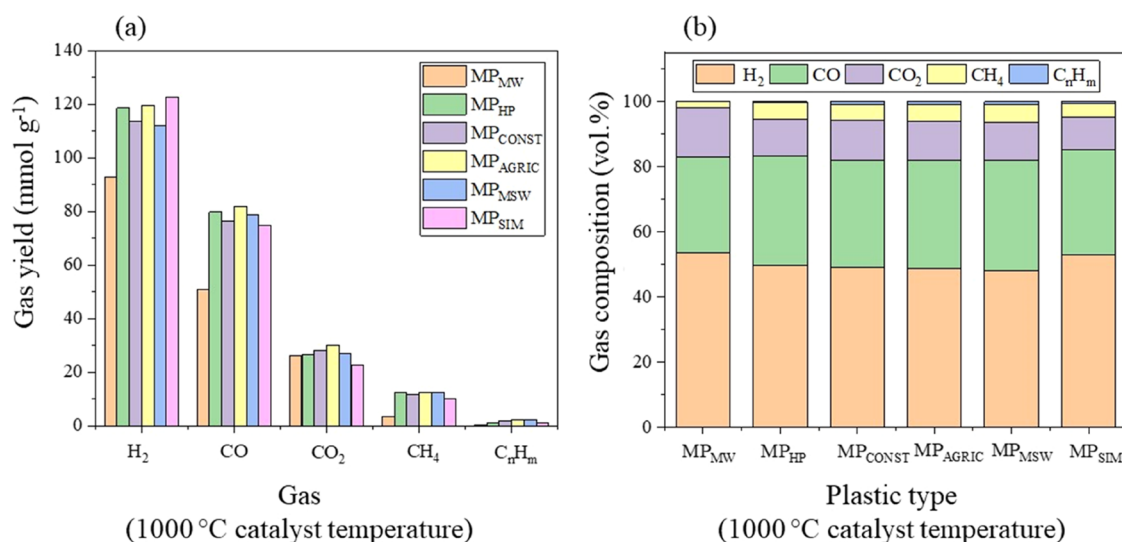


Figure 7. (a) Gas yield and (b) gas composition (vol.%) from pyrolysis–catalytic steam reforming of mixed waste plastics at a char catalyst temperature of 1000 °C.

H₂ concentration came from the steam reforming of hydrocarbons. The increase in H₂ concentration resulted in a slight decrease in CO content.

3.3. Pyrolysis–Catalytic Steam Reforming of Mixed Plastics. **3.3.1. Product Yields from Pyrolysis–Catalytic Steam Reforming of Mixed Plastics.** The product yield from pyrolysis–catalytic steam reforming of different mixed real-world waste plastics was investigated at a catalyst temperature of 1000 °C and a steam flow rate of 8 mL h⁻¹. The product yield, the mass of char that was reacted with steam, and the amount of reacted water are shown in Table 4. The gas yield from pyrolysis–catalytic steam reforming of MP_{MW} (mixed plastics from mineral water bottle packaging) was the lowest, at 30.61 wt %, mainly because mineral water containers were composed of PET. From the previous section on single plastics processing, it can be seen that PET was not fully converted into pyrolysis volatile components during pyrolysis, resulting in the production of a residual char of 17 wt %. Alvarez et al.⁴² reported that the presence of PET increased the final amount of solid residue in the pyrolysis/gasification of a biomass and plastic mixture with the aim of producing hydrogen. The agricultural waste plastic (MP_{AGRIC}) used in this study was mainly comprised of PE and PP, which resulted in the highest gas yield at 43.47 wt %. The mixed plastics from household wastes (excluding PET) (MP_{HP}) and the mixed plastics from construction sites (MP_{CONST}) gave a similar gas yield at around 42 wt %. In contrast, the gas yield of mixed plastics from municipal solid waste (MP_{MSW}) and simulated mixed plastics (MP_{SIM}) was lower, which reflected the effect of the presence of significant quantities of PET in the MP_{MSW} and MP_{SIM} samples. The pyrolysis–catalytic steam reforming of mixed plastics (MP_{MW}) containing PET consumed more of the tire char carbon by steam–char gasification than other mixed plastics. This was because the oxygenated compounds in the volatiles produced from the pyrolysis of PET promoted the reactions of carbon to generate carbon oxides.

3.3.2. Gas Yields from Pyrolysis–Catalytic Steam Reforming of Mixed Plastics. Figure 7a shows the individual gas yields from the pyrolysis–catalytic steam reforming of the different mixed plastics. The difference in individual gas yield was mainly caused by the different proportions of the single plastics

that made up the plastic mixtures. For example, the main component produced from the processing of the mixed plastics from mineral water bottles (MP_{MW}) was PET, which had the lowest H₂ yield of 92.81 mmol g_{plastic}⁻¹, which was very similar to the H₂ yield produced from processing the single plastic PET under the same conditions. The simulated mixture of plastics prepared to represent municipal solid waste plastics (MP_{SIM}) had the highest H₂ yield at 122.6 mmol g_{plastic}⁻¹, which was related to its high fraction of LDPE (41 wt %) and HDPE (19 wt %). In this study, part of the CO₂ in the pyrolysis gas came from the water gas shift reaction (eq 10) and part came from the reaction between steam and the carbon in the tire char (eq 12). For mixed plastics containing PET, some CO₂ came from oxygenated compounds (C_nH_mO_k) via the steam reforming reaction (eq 9). C_nH_mO_k was the primary pyrolysis volatile from MP_{MW}, while CH₄ and C_nH_m were the main pyrolysis volatiles of the other mixed plastic wastes. Different proportions of the individual plastics that made up the mixed plastics led to varying amounts of pyrolysis volatiles, so the yields of CH₄ and C_nH_m were slightly different after steam reforming.

3.3.3. Volumetric Gas Composition from Pyrolysis–Catalytic Steam Reforming of Mixed Plastics. The volumetric gas composition for pyrolysis–catalytic steam reforming of different real-world waste plastics is shown in Figure 7b. As can be seen from Figure 7b, the H₂ concentration ranged from 48.2 to 53.5 vol %. The H₂ concentration from pyrolysis–catalytic steam reforming of mineral water bottle waste plastics (MP_{MW}) was the highest, at around 53.5 vol %, followed by the prepared simulated mixture of waste plastics (MP_{SIM}) at 52.9 vol %, which is related to the presence of PET. Under the same conditions, the H₂ concentration in the catalytic pyrolysis gas of PET was 52.4 vol %. H₂ concentration from the other mixed plastics was similar, at around 49 vol %. As for the CO concentration, the pyrolysis gas from MP_{MW} contained the lowest content of CO (29.4 vol %) and the highest content of CO₂ (15.1 vol %). This was because oxygenated compounds (C_nH_mO_k), a significant component of MP_{MW} pyrolysis volatiles, generated CO₂ after steam reforming. The other five mixed plastics produced a gas that contained about 33 vol % CO. The low content of C_nH_m in all of the different mixed

Table 5. Theoretical and Experimental Hydrogen Yield in Relation to the Single and Mixed Plastics^a

plastic	theoretical H ₂ yield (mmol g _{plastic} ⁻¹)	char catalyst temperature 900 °C		char catalyst temperature 1000 °C	
		experimental ^a (plastics) (%)	experimental ^b (plastics + char) (%)	experimental ^a (plastics) (%)	experimental ^b (plastics + char) (%)
HDPE	207.89	29.79	18.28	59.83	36.71
LDPE	220.24	31.01	19.45	60.43	37.90
PP	218.80	28.10	17.58	55.62	34.80
PS	179.31	34.61	20.00	62.31	36.01
PET	98.12	49.48	21.20	92.91	39.80
MP _{SIM}	193.29			63.43	37.81
MP _{MW}	114.11			81.33	37.87
MP _{HP}	184.39			64.33	37.61
MP _{CONST}	189.49			60.02	35.50
MP _{AGRIC}	184.59			64.78	37.90
MP _{MSW}	184.55			60.61	35.45

^aNomenclature: Percentage of the experimental H₂ yield to theoretical H₂ yield from plastics. ^bPercentage of the experimental H₂ yield to theoretical H₂ yield from plastics plus char.

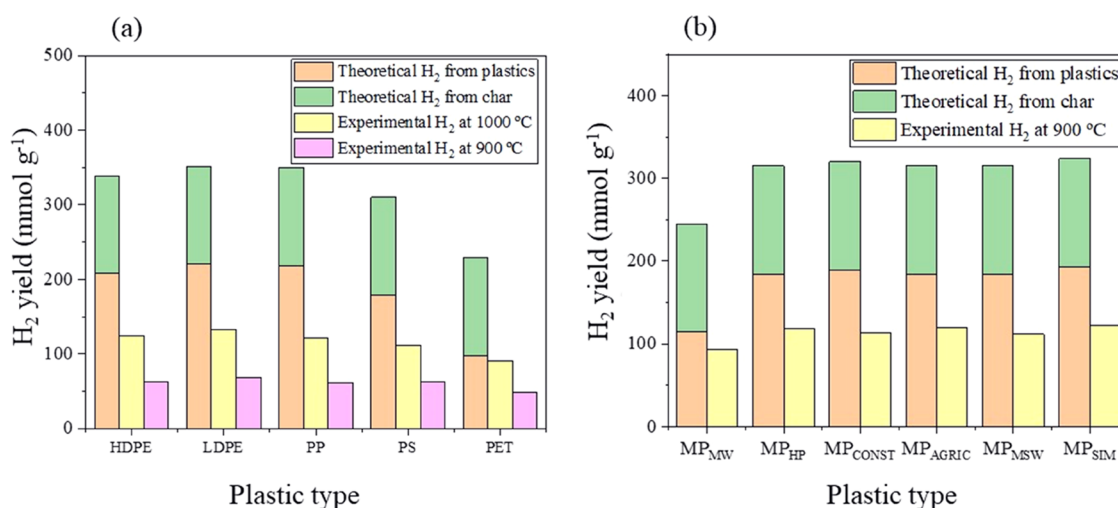


Figure 8. Maximum theoretical hydrogen production derived from the waste plastic and also the tire char in relation to the reported experimental data for (a) the single waste plastics catalytically steam-reformed at 900 and 1000 °C and (b) the industrial and commercial mixed waste plastics catalytically steam-reformed at 1000 °C.

waste plastics indicated that the tire char played a crucial role in the catalytic steam reforming reaction.

3.4. Maximum Theoretical Hydrogen Yield. The concept of the maximum theoretical hydrogen potential was introduced by Czernik and French¹⁹ in relation to hydrogen production from waste plastics via the pyrolysis–steam reforming process. They suggested that the maximum potential hydrogen production includes both steam reforming (eqs 7–9) and water gas shift reactions (eq 10). Therefore, it is assumed that all of the hydrocarbons derived from plastic pyrolysis are converted to carbon dioxide and hydrogen. Table 5 shows the calculated maximum theoretical hydrogen production for the single and mixed waste plastics based on the elemental compositions of the plastics shown in Table 1.

In addition, the steam gasification of tire char also contributed to the hydrogen yield (eqs 11–13) via the water gas shift reaction of the steam with the evolved carbon oxides. The calculated theoretical maximum hydrogen yield from the tire char was calculated from its elemental composition and the char gasification reactions and was found to be 130.93 mmol g_{char}⁻¹. Figure 8 shows the calculated maximum theoretical hydrogen production of the single (Figure 8a) and mixed waste plastics (Figure 8b), including tire char steam gasification, in

relation to the experimental hydrogen yield data from the pyrolysis–catalytic steam reforming process with the tire char catalyst. In addition, Table 5 shows the percentage of the maximum theoretical hydrogen production achieved experimentally using the pyrolysis–catalytic steam reforming process with the tire char catalyst; the data show the maximum theoretical yield achieved at 900 °C and 1000 °C catalyst temperatures and in terms of the percentage in relation to the maximum theoretical yield from the plastics only and also from the plastics plus char.

The yield of hydrogen from the single plastics was 68.29 mmol g_{plastic}⁻¹ for LDPE at a catalyst temperature of 900 °C (Figure 4a). From Table 5, this represents 31.01% of the maximum theoretical hydrogen production that could be produced from LDPE and 19.45% in relation to the maximum theoretical hydrogen yield from plastics plus char. However, when the temperature of the tire char catalyst was increased to 1000 °C (Figure 4b), the percentage theoretical hydrogen yield achieved from the LDPE was 133.10 mmol g_{plastic}⁻¹, representing 60.43% of the theoretical yield from LDPE and 37.90% if the theoretical hydrogen yield from the char is also included. The highest theoretical hydrogen yield was found with PET at 1000 °C char catalyst temperature, where 92.91%

was achieved as the percentage of the theoretical hydrogen yield from PET.

Figure 8b and Table 5 show the theoretical hydrogen yields in relation to the mixed commercial and industrial waste plastics for experiments undertaken at a catalyst temperature of 1000 °C. The highest hydrogen yield experimentally was from the mixed plastic mixture prepared to represent the plastic mixture in municipal solid waste (MP_{SIM}) at 122.6 mmol g_{plastic}⁻¹ (Figure 7a). This represented 63.43% of the maximum theoretical hydrogen yield (Table 5). This was similar to the other mixed waste plastics between 60.02 and 64.78% of the theoretical maximum hydrogen yield for the mixed plastic wastes from MP_{CONST}, MP_{HP}, MP_{MSW}, and MP_{AGRIC}. The highest theoretical hydrogen yield achieved was in relation to the mixed plastic waste containing mineral water bottles (MP_{MW}) at 81.33%, which is consistent with the high content of PET in this waste stream. Although the conversion is high, the actual hydrogen yield produced is low at 92.81 mmol g_{plastic}⁻¹, (Figure 7a).

This work has shown that hydrogen-rich syngas can be successfully produced in high yield from different common single plastics and also from a range of high-volume commercial and industrial mixed waste plastics. The yields and composition of hydrogen and syngas produced from the mixed waste plastics are informed from the amounts of single plastics comprising their composition in the plastic mixture. The advantage of using mixed plastics produced from specific commercial and industrial sectors is the comparatively known heterogeneity and the controlled collection regime. The focus of the work reported here also investigated a reforming catalyst comprised of tire char that was produced from a waste material, namely, waste tires. The tire char catalyst was chosen as a reforming catalyst based on its content of transition metals, commonly investigated as active reforming catalyst metals (Fe, Zn, Cu, Co).⁹ But, in addition, the tire char was chosen to act as a reactant to produce further yields of H₂ via the reaction of the char with steam via water–gas reactions. In addition, the reaction of the steam and char would produce CO through water–gas and Boudouard reactions which could further react with steam to produce even more H₂ via the water gas shift reaction. For further development of the process, a continuous operation system would need to be developed rather than the batch process reported here. Such continuous processes have been developed based on fluidized bed reaction systems.^{14,19} Also, since the char catalyst is a reactant, it is used up or “sacrificed” during the reforming process. Consequently, a balance between reacting the char and maintaining some form of catalyst activity would have to be determined. A full techno-economic assessment would also have to be carried out.^{43,44}

4. CONCLUSIONS

In this work, a range of single plastics and mixed commercial and industrial waste plastics have been investigated for the production of hydrogen using a pyrolysis–catalytic steam reforming process with a char catalyst derived from waste tires. Hydrogen was produced from the process from both the catalytic steam reforming of the plastics pyrolysis volatiles and also from the “sacrificial” steam gasification of the char. The highest yield of gas obtained at a char catalyst temperature of 900 °C was from the processing of the polyolefin plastics (HDPE, LDPE, and PP), which was between 36.84 and 39.08 wt % (based on the input of plastic, reacted steam, and char

gasification). Much lower gas yields were obtained for PS (21.27 wt %) and PET (18.71 wt %). However, if the mass of gas was calculated based on the mass of input plastic only, then very high gas yields are obtained because of the contribution from char gasification and reacted water; for example, the gas yield from LDPE on this basis was 356.03 wt %. The influence of increasing the char catalyst temperature from 900 to 1000 °C resulted in a large increase in total gas yield. For example, the gas yield from LDPE increased from 356.03 to 445.07 wt % (based on the mass of input plastic only). It is interesting and legitimate to present such high gas yields in terms of the yield from the plastics only since the other inputs to the process are water (steam) and tire pyrolysis char produced from a waste material, both of which are low cost. The product gas was largely composed (~80 vol %) of H₂ and CO, i.e., syngas, and increased significantly as the temperature of the char catalyst was raised. For example, the yield of H₂ from the processing of LDPE was 68.29 mmol g_{plastic}⁻¹ at 900 °C catalyst temperature, which increased to 133.10 mmol g_{plastic}⁻¹ at a catalyst temperature of 1000 °C. Lower H₂ yields were obtained for HDPE, PP, and PS at about 62 mmol g_{plastic}⁻¹, while the yield of PET was the lowest at 48.55 mmol g_{plastic}⁻¹ since PET produced a significant amount of residual char, and the gases produced from the pyrolysis of PET are largely CO and CO₂.

The pyrolysis–catalytic steam processing of the industrial and commercial mixed plastics in the presence of the tire char catalyst was influenced by the different proportions of the single plastics that made up the mixed plastics. For example, the main component of the mixed plastics from mineral water bottle waste (MP_{MW}) was PET, which had the lowest H₂ yield of 92.81 mmol g_{plastic}⁻¹, which was very similar to the H₂ yield of the single PET plastic at the same conditions. The simulated mixture of single plastics (MP_{SIM}) had the highest H₂ yield at 122.6 mmol g_{plastic}⁻¹ since the mixture had a high content of LDPE (41 wt %) and HDPE (19 wt %).

The maximum theoretical potential hydrogen production was calculated from the plastics based on plastic-derived pyrolysis volatile gases and steam reforming, water gas shift reactions, and char steam gasification reactions. For example, at a tire catalyst temperature of 1000 °C, the maximum theoretical hydrogen production achieved was 60.43% based on reforming and water gas shift reactions and 37.90% if char gasification reactions are also included.

■ AUTHOR INFORMATION

Corresponding Author

Paul T. Williams – School of Chemical & Process Engineering, University of Leeds, Leeds LS2 9JT, U.K.; orcid.org/0000-0003-0401-9326; Phone: #44 1133432504; Email: p.t.williams@leeds.ac.uk

Authors

Yukun Li – School of Chemical & Process Engineering, University of Leeds, Leeds LS2 9JT, U.K.
Mohamad A. Nahil – School of Chemical & Process Engineering, University of Leeds, Leeds LS2 9JT, U.K.

Complete contact information is available at:
<https://pubs.acs.org/10.1021/acs.energyfuels.3c00499>

Notes

The authors declare no competing financial interest.

ACKNOWLEDGMENTS

Y.L. was awarded a China Scholarship Council—University of Leeds scholarship to carry out the research, which is gratefully acknowledged.

REFERENCES

- (1) OECD *Plastics Flows and their Impacts on the Environment, in Global Plastics Outlook: Economic Drivers, Environmental Impacts and Policy Options*; OECD Publishing: Paris, France; 2022.
- (2) PlasticsEurope *The Circular Economy for Plastics; A European Overview*; Plastics Europe: Brussels, Belgium, 2022.
- (3) EEA *Plastics, The Circular Economy and Europe's Environment: A Priority for Action*, European Environment Agency: Copenhagen, Denmark, 2020.
- (4) IEA *International Energy Agency (IEA) Global Hydrogen Review*; International Energy Agency: Paris, France, 2022.
- (5) Lopez, G.; Artetxe, M.; Amutio, M.; Alvarez, J.; Bilbao, J.; Olazar, M. Recent advances in the gasification of waste plastics. A critical overview. *Renewable Sustainable Energy Rev.* **2018**, *82*, 576–596.
- (6) Dai, L.; Zhou, N.; Lv, Y.; Cheng, Y.; Wang, Y.; Liu, Y.; Cobb, K.; Chen, P.; Lei, H.; Ruan, R. Pyrolysis technology for plastic waste recycling: A state-of-the-art review. *Prog. Energy Combust. Sci.* **2022**, *93*, No. 101021.
- (7) Yang, R. X.; Jan, K.; Chen, C. T.; Chen, W. T.; Wu, K.C.W. Thermochemical conversion of plastic waste into fuels, chemicals, and value-added materials: A critical review and outlooks. *ChemSusChem* **2022**, *15*, No. e202200171.
- (8) Midilli, A.; Kucuk, H.; Haciosmanoglu, M.; Akbulut, U.; Dincer, I. A review on converting plastic wastes into clean hydrogen via gasification for better sustainability. *Int. J. Energy Res.* **2022**, *46*, 4001–4032.
- (9) Santamaria, L.; Lopez, G.; Fernandez, E.; Cortazar, M.; Arregi, A.; Olazar, M.; Bilbao, J. Progress on catalyst development for the steam reforming of biomass and waste plastics pyrolysis volatiles: a review. *Energy Fuels* **2021**, *35*, 17051–17084.
- (10) Williams, P. T. Hydrogen and carbon nanotubes from pyrolysis-catalysis of waste plastics: A review. *Waste Biomass Valorization* **2021**, *12*, 1–28.
- (11) Jiang, Y.; Li, X.; Li, C.; Zhang, L.; Zhang, S.; Li, B.; Wang, S.; Hu, X. Pyrolysis of typical plastics and coupled with steam reforming of their derived volatiles for simultaneous production of hydrogen-rich gases and heavy organics. *Renewable Energy* **2022**, *200*, 476–491.
- (12) Cortazar, M.; Gao, N.; Quan, C.; Suarez, M. A.; Lopez, G.; Orozco, S.; Santamaria, L.; Amutio, M.; Olazar, M. Analysis of hydrogen production potential from waste plastics by pyrolysis and in line oxidative steam reforming. *Fuel Process. Technol.* **2022**, *225*, No. 107044.
- (13) Yao, D.; Yang, H.; Chen, H.; Williams, P. T. Investigation of nickel-impregnated zeolite catalysts for hydrogen/syngas production from the catalytic reforming of waste polyethylene. *Appl. Catal., B* **2018**, *227*, 477–487.
- (14) Barbarias, I.; Lopez, G.; Alvarez, J.; Artetxe, M.; Arregi, A.; Bilbao, J.; Olazar, M. A sequential process for hydrogen production based on continuous HDPE fast pyrolysis and in-line steam reforming. *Chem. Eng. J.* **2016**, *296*, 191–198.
- (15) Sehested, J. Four challenges for nickel steam-reforming catalysts. *Catal. Today* **2006**, *111*, 103–110.
- (16) Wu, C.; Williams, P. T. Investigation of Ni-Al, Ni-Mg-Al and Ni-Cu-Al catalyst for hydrogen production from pyrolysis–gasification of polypropylene. *Appl. Catal., B* **2009**, *90*, 147–156.
- (17) Wu, C.; Williams, P. T. Hydrogen production by steam gasification of polypropylene with various nickel catalysts. *Appl. Catal., B* **2009**, *87*, 152–161.
- (18) Yao, D.; Yang, H.; Chen, H.; Williams, P. T. Co-precipitation, impregnation and so-gel preparation of Ni catalysts for pyrolysis-catalytic steam reforming of waste plastics. *Appl. Catal., B* **2018**, *239*, 565–577.
- (19) Czernik, S.; French, R. J. Production of hydrogen from plastics by pyrolysis and catalytic steam reform. *Energy Fuels* **2006**, *20*, 754–758.
- (20) Aminu, I.; Nahil, M. A.; Williams, P. T. In *High-Yield Hydrogen from Thermal Processing of Waste Plastics*, Proceedings of the Institution of Civil Engineers-Waste and Resource Management; Thomas Telford Ltd, 2022; pp 3–13.
- (21) Wu, C.; Williams, P. T. Pyrolysis-gasification of post consumer municipal solid plastic waste for hydrogen production. *Int. J. Hydrogen Energy* **2010**, *35*, 949–957.
- (22) Zhang, Y.; Huang, J.; Williams, P. T. Fe–Ni–MCM-41 catalysts for hydrogen-rich syngas production from waste plastics by pyrolysis–catalytic steam reforming. *Energy Fuels* **2017**, *31*, 8497–8504.
- (23) El-Rub, Z. A.; Bramer, E. A.; Brem, G. Experimental comparison of biomass chars with other catalysts for tar reduction. *Fuel* **2008**, *87*, 2243–2252.
- (24) Yao, D.; Hu, Q.; Wang, D.; Yang, H.; Wu, C.; Wang, X.; Chen, H. Hydrogen production from biomass gasification using biochar as a catalyst/support. *Bioresour. Technol.* **2016**, *216*, 159–164.
- (25) Zhang, S.; Asadullah, M.; Dong, L.; Tay, H.-L.; Li, C.-Z. An advanced biomass gasification technology with integrated catalytic hot gas cleaning. Part II: Tar reforming using char as a catalyst or as a catalyst support. *Fuel* **2013**, *112*, 646–653.
- (26) Wang, N.; Chen, D.; Arena, U.; He, P. Hot char-catalytic reforming of volatiles from MSW pyrolysis. *Appl. Energy* **2017**, *191*, 111–124.
- (27) Jiang, L.; Hu, S.; Wang, Y.; Su, S.; Sun, L.; Xu, B.; He, L.; Xiang, J. Catalytic effects of inherent alkali and alkaline earth metallic species on steam gasification of biomass. *Int. J. Hydrogen Energy* **2015**, *40*, 15460–15469.
- (28) Wang, D.; Li, B.; Yang, H.; Zhao, C.; Yao, D.; Chen, H. Influence of biochar on the steam reforming of biomass volatiles: effects of activation temperature and atmosphere. *Energy Fuels* **2019**, *33*, 2328–2334.
- (29) Liu, Y.; Paskevicius, M.; Wang, H.; Parkinson, G.; Veder, J.-P.; Hu, X.; Li, C.-Z. Role of O-containing functional groups in biochar during the catalytic steam reforming of tar using the biochar as a catalyst. *Fuel* **2019**, *253*, 441–448.
- (30) Al-Rahbi, A. S.; Williams, P. T. Hydrogen-rich syngas production and tar removal from biomass gasification using sacrificial tyre pyrolysis char. *Appl. Energy* **2017**, *190*, 501–509.
- (31) Delgado, C.; Barruetabeña, L.; Salas, O.; Wolf, O. *Assessment of the Environmental Advantages and Drawbacks of Existing and Emerging Polymers Recovery Processes*; Institute for Prospective Technological Studies, Joint Research Centre, European Commission, 2007.
- (32) Al-Rahbi, A. S.; Williams, P. T. Decomposition of biomass gasification tar model compounds over waste derived tyre pyrolysis char. *Waste Disposal Sustainable Energy* **2022**, *4*, 75–89.
- (33) Williams, P. T. Pyrolysis of waste tyres: a review. *Waste Manage.* **2013**, *33*, 1714–1728.
- (34) Zhou, Q.; Zarei, A.; De Girolamo, A.; Yan, Y.; Zhang, L. Catalytic performance of scrap tyre char for the upgrading of eucalyptus pyrolysis derived bio-oil via cracking and deoxygenation. *J. Anal. Appl. Pyrolysis* **2019**, *139*, 167–176.
- (35) Jones, I.; Preciado-Hernandez, J.; Zhu, M.; Zhang, J.; Zhang, Z.; Zhang, D. Utilisation of spent tyre pyrolysis char as activated carbon feedstock: The role, transformation and fate of Zn. *Waste Manage.* **2021**, *126*, 549–558.
- (36) Williams, P. T.; Williams, E. A. Interaction of plastics in mixed-plastics pyrolysis. *Energy Fuels* **1999**, *13*, 188–196.
- (37) Barbarias, I.; Lopez, G.; Artetxe, M.; Arregi, A.; Bilbao, J.; Olazar, M. Valorisation of different waste plastics by pyrolysis and in-line catalytic steam reforming for hydrogen production. *Energy Convers. Manage.* **2018**, *156*, 575–584.
- (38) Wu, C.; Williams, P. T. Pyrolysis–gasification of plastics, mixed plastics and real-world plastic waste with and without Ni–Mg–Al catalyst. *Fuel* **2010**, *89*, 3022–3032.

(39) Franco, C.; Pinto, F.; Gulyurtlu, I.; Cabrita, I. The study of reactions influencing the biomass steam gasification process. *Fuel* **2003**, *82*, 835–842.

(40) Chaudhari, S.; Bej, S.; Bakhshi, N.; Dalai, A. Steam gasification of biomass-derived char for the production of carbon monoxide-rich synthesis gas. *Energy Fuels* **2001**, *15*, 736–742.

(41) Wender, I. Reactions of synthesis gas. *Fuel Process. Technol.* **1996**, *48*, 189–297.

(42) Alvarez, J.; Kumagai, S.; Wu, C.; Yoshioka, T.; Bilbao, J.; Olazar, M.; Williams, P. T. Hydrogen production from biomass and plastic mixtures by pyrolysis-gasification. *Int. J. Hydrogen Energy* **2014**, *39*, 10883–10891.

(43) Al-Qadri, A. A.; Ahmed, U.; Abdul Jameel, A. G.; Zahid, U.; Ahmad, N.; Shahbaz, M.; Nemitallah, M. A. Technoeconomic Feasibility of Hydrogen Production from Waste Tires with the Control of CO₂ Emissions. *ACS Omega* **2022**, 48075–48086.

(44) Al-Qadri, A. A.; Ahmed, U.; Abdul Jameel, A. G.; Zahid, U.; Usman, M.; Ahmad, N. Simulation and Modelling of Hydrogen Production from Waste Plastics: Technoeconomic Analysis. *Polymers* **2022**, *14*, No. 2056.

Recommended by ACS

Hydrogen Production by Three-Stage (i) Pyrolysis, (ii) Catalytic Steam Reforming, and (iii) Water Gas Shift Processing of Waste Plastic

Rayed Alshareef, Paul T. Williams, *et al.*

FEBRUARY 14, 2023
ENERGY & FUELS

[READ](#) 

Oxidative Fast Pyrolysis of High-Density Polyethylene on a Spent Fluid Catalytic Cracking Catalyst in a Fountain Confined Conical Spouted Bed Reactor

Santiago Orozco, Martin Olazar, *et al.*

NOVEMBER 17, 2022
ACS SUSTAINABLE CHEMISTRY & ENGINEERING

[READ](#) 

Characteristics of Air Gasification of 10 Different Types of Plastic in a Two-Stage Gasification Process

Yong-Seong Jeong, Joo-Sik Kim, *et al.*

MARCH 29, 2022
ACS SUSTAINABLE CHEMISTRY & ENGINEERING

[READ](#) 

Distilled Waste Plastic Oil as Fuel for a Diesel Engine: Fuel Production, Combustion Characteristics, and Exhaust Gas Emissions

Weerachai Arjharn, Ekarong Sukjit, *et al.*

MARCH 10, 2022
ACS OMEGA

[READ](#) 

[Get More Suggestions >](#)